RSC Advances

PAPER

View Article Online
View Journal | View Issue

Cite this: *RSC Adv.*, 2017, **7**, 41838

A superhydrophilic and underwater superoleophobic chitosan–TiO_2 composite membrane for fast oil-in-water emulsion separation†

Yanqing Du, [a] Yujiang Li *[a] and Tao Wu*[b]

Received 27th July 2017
Accepted 22nd August 2017

DOI: 10.1039/c7ra08266e

rsc.li/rsc-advances

Oil/water separation has become a worldwide challenge due to large volumes of industrial oily wastewater and frequent oil spill accidents, which constitute an enormous threat to human and biological safety. Herein, a superhydrophilic and underwater superoleophobic composite membrane was fabricated using the vacuum-assisted filtration technique of assembly of chitosan (CS) and titanium dioxide (TiO_2) on a cellulose acetate membrane for emulsified oil separation. The hydrophilic chitosan–TiO_2 (CST) composite and nanoscale hierarchical structure are beneficial for forming a water layer that can repel the infiltration of oil droplets into the membrane. The modified membrane demonstrated an excellent flux up to 6002.5 L m^{-2} h^{-1} for hexadecane-in-water emulsion, which is one order of magnitude higher than traditional filtration membranes. Furthermore, the separation efficiency for all of the emulsified oils is above 97%, indicating superior oil/water separation performance. Most importantly, the modified membrane can maintain underwater superoleophobicity even in corrosive aqueous media, including strongly acidic, strongly alkaline, and highly saline solutions. It is expected that the chitosan–TiO_2 composite membrane can be potentially useful in treating oily wastewater from industry and daily life.

1. Introduction

With the development of the world economy, large volumes of oily wastewater are produced by the food, pharmaceutical, petrochemical, textile, metal finishing, and steel industries and frequent oil spill accidents, which bring severe environmental pollution.[1–3] Due to the severe negative influences of oily wastewater on the environment and human life, functional materials that can separate oily wastewater efficiently are highly sought by many researchers. Conventional oil/water separation techniques, such as centrifugation, skimming, coagulation–flocculation, air flotation and gravity separation, are restricted by high energy input, complex separation steps, generation of secondary pollutants, and low separation efficiency in treating oil-in-water emulsions.[4–6] However, membrane separation technology has been acknowledged as an advanced method that is environmentally friendly, economical, highly efficient, possesses a small footprint, and is easy to scale up compared to other techniques.[7,8]

There are two types of oil/water separation membranes that have been utilized to separate oily wastewater, including "oil-removing" and "water-removing".[9] In recent years, "oil-removing" membranes with a superhydrophobic and superoleophilic surface have attracted widespread attention. The "oil-removing" membrane allows the oil droplets to filter through, be absorbed by, or spread over the membrane surface, and the water is repelled. For example, Li *et al.* coated silica particles on stainless steel mesh to fabricate a highly hydrophobic and superoleophilic surface for oil/water separation.[10] Cao *et al.* reported a highly hydrophobic mesh coating with adhesive polydopamine and *n*-dodecyl mercaptan for oil/water separation.[11] However, during the oil removal process, these superoleophilic membranes are easily polluted or even blocked by adhered or adsorbed oils due to their intrinsic oleophilic property, which induces a rapid decrease in flux, separation efficiency, and membrane life. Furthermore, it is difficult to remove these adhered or adsorbed oils. Cleaning oils during the post-treatment process also results in second pollution, as well as a waste of both oleophilic materials and oils.[12,13] In contrast, "water-removing" membrane with superhydrophilic and underwater superoleophobic materials could overcome these disadvantages, and constitutes an attractive approach to solve the long-term use and effective oily wastewater separation problems.[14] In addition, during the oily water separation process, the oil-adhesion force of the underwater superoleophobic membrane is

[a]*Shandong Provincial Key Laboratory of Water Pollution Control and Resource Reuse, School of Environmental Science and Engineering, Shandong University, Jinan, 250100, PR China. E-mail: yujiang@sdu.edu.cn*

[b]*Key Laboratory of Colloid and Interface Science of Education Ministry, Shandong University, Jinan, 250100, PR China. E-mail: wutao@sdu.edu.cn*

† Electronic supplementary information (ESI) available. See DOI: 10.1039/c7ra08266e

extremely low, preventing the membrane from fouling by oil, which makes the membrane recyclable.

Recently, many research groups have fabricated underwater superoleophobic membranes for oil/water separation. As a typical example, Liu *et al.* reported a polydopamine-coated reduced graphene oxide membrane with high separation efficiency for multiple types of oil-in-water emulsions.[15] Lin *et al.* fabricated a TiO_2 nanocluster-based mesh by a strategic solvothermal method *in situ* emulsion separation with an ultrafast and efficient step.[16] Zhao *et al.* reported a facile free-standing graphene oxide-palygorskite (GOP) nanohybrid membrane with high separation efficiency and antifouling property.[17] However, most of these membranes were not chemically stable in corrosive conditions, especially under a strong acid or alkali environment, which seriously limited the application of the membrane. Therefore, to develop a stable underwater superoleophobic membrane which can adapt to sharp corrosive conditions, possesses high oil/water separation flux, and is economically feasible is of paramount significance.

Chitosan (CS), as a nontoxic, naturally biodegradable, and biocompatible polysaccharide derived from the deacetylation of chitin has become an attractive polymer with high hydroxyl and amino functional groups present on the surface.[18–23] Moreover, the amines of chitosan are protonated under acidic conditions to confer chitosan positive charges and membrane-forming properties.[24] Titanium dioxide (TiO_2) nanoparticles with a superhydrophilic surface, high safety and stability, wide availability, low cost, and self-cleaning surface, have been regarded as the optimal candidate material for effective oil/water separation.[25,26] In this work, we expect to develop a superhydrophilic and underwater superoleophobic membrane by the filtration technique under a vacuum filtration device based on chitosan and TiO_2 on a cellulose acetate membrane for the separation of oil-in-water emulsions. The resulting modified chitosan–TiO_2 (CST) composite membrane is not only excellent for oil-in-water emulsions separation with high separation efficiency and flux, but also suitable for large-scale production. The modified membrane shows outstanding underwater superoleophobicity even in strongly acidic, alkaline, and saline environments. The current work may contribute substantially to the development of efficient and inexpensive oil/water separation membranes for practical applications.

2. Experimental

2.1 Materials

The cellulose acetate membrane (CAM, pore size 220 nm, φ 47 mm) utilized in this work was purchased from Beijing Safelab Technology, Ltd., Beijing, China. TiO_2 nanoparticles (anatase, hydrophilic, 60 nm, 99.8%) (Macklin Biochemical Technology Co., Ltd., Shanghai, China), hexadecane (Tokyo Chemical Industry Co., Ltd., Tokyo, Japan), glutaraldehyde (Tianjin Damao Chemical Reagent Co., Ltd., Tianjin, China), carbon tetrachloride (Tianjin Guangfu Fine Chemical Research Institute, Tianjin, China), octane (Aladdin, China), and sodium dodecyl sulfate (SDS, Tianjin Fengchuan Chemical Reagent Technologies Co., Ltd., Tianjin, China) were used as purchased. Chitosan, petroleum ether, toluene, acetic acid, and 1,2-dichloroethane were purchased from Sinopharm Chemical Reagent Co., Ltd., Shanghai, China and used as received. Deionized (DI) water (conductivity 18.2 MΩ cm^{-1}) was achieved from a Milli-Q system (Flom, China).

2.2 Fabrication of the CST and CS modified membrane

The CST and CS modified membranes were fabricated by the filtration technique under a vacuum filtration device. Typically, 30 mg of chitosan was dissolved in 100 mL 1% (v/v) of acetic acid solution, and then 0.2 mL of glutaraldehyde was added into this solution. Subsequently, the prepared solution was stirred gently at room temperature for 12 h to obtain a homogenous solution. TiO_2 nanoparticles (5 mg, 20 mg, and 35 mg) were ultrasonically dispersed in 50 mL deionized water. To fabricate the CST modified membrane, the resulting chitosan homogenous solution (5 mL) was vacuum-filtrated on one piece of clean cellulose acetate membrane firstly, and then 5 mL TiO_2 solution with different concentrations was vacuum-filtrated on the CS-coated membrane. The membrane was further dried at 40 °C in an oven for 6 h, and then the resulting membrane was washed with deionized water, and further dried at 40 °C for 2 h. Due to the mass ratio of CS and TiO_2, the modified CST membranes were denoted as CST (3 : 1), CST (3 : 4) and CST (3 : 7), respectively. The chitosan was 0.12 mg cm^{-2} for each modified membrane. In addition, the TiO_2 content for CST (3 : 1) membrane, CST (3 : 4) membrane and CST (3 : 7) membrane was 0.04, 0.16, 0.28 mg cm^{-2}, respectively. Similar to the CST modified membrane, the CS modified membrane was fabricated by pouring chitosan homogenous solution (5 mL) on the cellulose acetate membrane. The resulting membrane was further dried at 40 °C in an oven for 6 h, then washed with deionized water, after which the membrane was further dried at 40 °C in an oven for 2 h.

2.3 Preparation of the oil-in-water emulsions

Different kinds of surfactant-stabilized oil-in-water emulsions (hexadecane-in-water, octane-in-water, petroleum ether-in-water, and toluene-in-water) were prepared by adding 1.5 g of oil in 1 L of deionized water, and then mixed with 0.05 g sodium dodecyl sulfate (SDS) as the emulsifier, followed by stirring the mixture by a homogenizer (HG-15D, DAIHAN Scientific Co., Ltd., Korea) at 10 000 rpm for 10 min to produce a milky solution. All of the emulsions were stable at room temperature for hours and were used for oil/water separation immediately.

2.4 Oil-in-water emulsion separation

The emulsion separation tests were performed by a vacuum filter apparatus (Fig. S1†) equipped with the modified membrane (separation area is 12.56 cm^2). The membrane was wetted by water prior to oil-in-water emulsion separation. For each separation process, 50 mL of the prepared oil-in-water emulsion was poured into the upper filtration cup under a pressure difference of 0.09 MPa. The water permeated through the membrane quickly and was collected into the container, and the oil content in the collected water was determined by an

infrared spectrometer oil content analyzer (Oil 460, Beijing China Invent Instrument Tech. Co., Ltd., Beijing, China). After each cycle, the membrane was washed with deionized water, and then used for the next cycle until the membrane was completely blocked.

2.5 Characterization

The morphology of each membrane surface was observed using by scanning electron microscopy (SEM, JEOL JSM-6700F, Japan) and an energy dispersive X-ray spectroscopy (EDS) detector attached to the SEM was used to examine the elements distribution of the membrane surface. Contact angles (CA), including water contact angle (WCA) in air and underwater oil contact angle (OCA), were conducted on an interfacial rheometer (Tracker, IT Concept, France). To measure the WCA, water droplet (2 μL) was directly dropped onto the membrane surface using a microsyringe. When measuring the OCA, the membranes were first fixed on a glass slide and then wetted by water. The glass slide was put into a self-designed system including a transparent polycarbonate container serving as the water reservoir. 2 μL of oil droplet (1,2-dichloroethane) was carefully dropped on the membrane surface. The CA was obtained by measuring three different positions, and then the average value was calculated. Optical microscope images of oil-in-water emulsions were taken with a fluorescent microscope (Eclipse E200, Nikon Corporation, Japan). Dynamic light scattering (DLS, BI-200SM/BI-9000, Brookhaven, USA) was utilized to examine the oil droplet sizes of the oil-in-water emulsions. The surface roughness of the modified membrane was characterized utilizing atomic force microscopy (AFM, Bruker, USA) under tapping mode. The chemical compositions of the membranes were obtained by X-ray photoelectron spectroscopy (XPS, Thermo ESCALAB 250XI, USA).

3. Results and discussion

3.1 Preparation and surface morphology characterization of the modified membranes

The fabrication of CST membranes by the vacuum-assisted filtration technique was schematically presented in Fig. 1. The protonated amine group of chitosan is positively charged, and it can adhere well to the cellulose acetate membrane. The amino group of chitosan can react with the aldehyde group of glutaraldehyde to form a network copolymer.[27] Chitosan (1.5 mg) was first filtered to the pristine cellulose acetate membrane, enhancing the hydrophilic property of the modified membrane due to the existence of hydroxyl and amino functional groups on the chitosan. And then 5 mL TiO_2 solution with different concentrations was vacuum-filtrated on the CS-coated membrane. Herein, TiO_2 nanoparticles had nanoscale roughness and ensured good superhydrophilicity and underwater superoleophobicity. Moreover, TiO_2 nanoparticles could be closely deposited on the surface of chitosan through electrostatic interactions.[28]

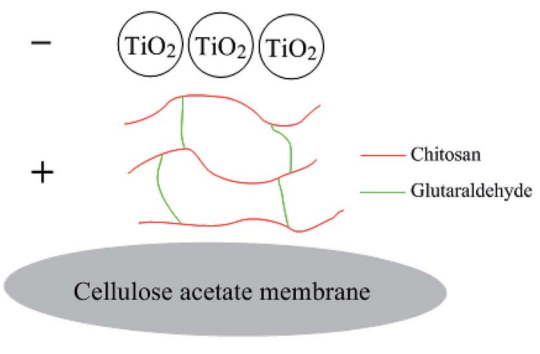

Fig. 1 Schematic illustration of the preparation procedure for the chitosan–TiO_2 composite membrane by the vacuum-assisted filtration technique.

To achieve advanced performance of effective oil/water separation, a membrane with superior oil resistance and water-spreading velocity is crucial. As is well-known, both geometrical structure and chemical composition influence the wettability of solid surfaces.[29–32] In this work, TiO_2 nanoparticles with a nanoscale hierarchical structure is critical for superhydrophilicity based on Cassie–Baxter theory.[33] The scanning electron microscope (SEM) images of pristine and modified membranes by chitosan and TiO_2 were depicted in Fig. 2. As clearly presented in Fig. 2a, the pristine cellulose acetate membrane exhibited an abundant porous structure with a relatively smooth and clean surface. However, after coating a layer of chitosan, we found that the porous structure of the pristine cellulose acetate membrane was preserved, and some nanostructures were formed on the surface of the membrane framework (Fig. 2b). Then, with the increase of TiO_2, the hydrophilic nanoparticles on the CST membrane increased, while the effective pore size decreased correspondingly (Fig. 2c–e), which is advantageous for the demulsification of emulsified oil containing small oil droplets. As shown in Fig. 2d, when the TiO_2 nanoparticles were increased to 20 mg, a layer of hydrophilic TiO_2 completely covered the membrane surface and filled the membrane pores. In addition, it can be seen from the membrane surface that the TiO_2 nanoparticles aggregated together to form a rough surface. With further increase of the content of TiO_2, the surface morphology of the modified membrane exhibited no apparent change (Fig. 2e).

To prevent membrane fouling, both chemical composition and hierarchical micro/nanostructures of membranes are two important factors. As is shown in Fig. 2f, root-mean-square roughness (R_q) was obtained by the AFM image of the membrane to determine roughness. We chose a porous cellulose acetate membrane with 3D pores as the skeleton or support for the coating materials. The AFM image showed that the pristine cellulose acetate membrane exhibited an R_q of 95.6 nm (Fig. S2a†). We deposited 1.5 mg of chitosan onto the pristine cellulose acetate membrane by vacuum filtration, and found that the roughness of the CS modified membrane was increased as the R_q was 108.67 nm (Fig. S2b†). When we added 0.5 mg hydrophilic TiO_2 nanoparticles onto the membrane, the R_q value decreased to 104.30 nm as presented in Fig. S2c,† indicating the loss of roughness with the coating of TiO_2. As we further increased the hydrophilic TiO_2 nanoparticles to 2 mg,

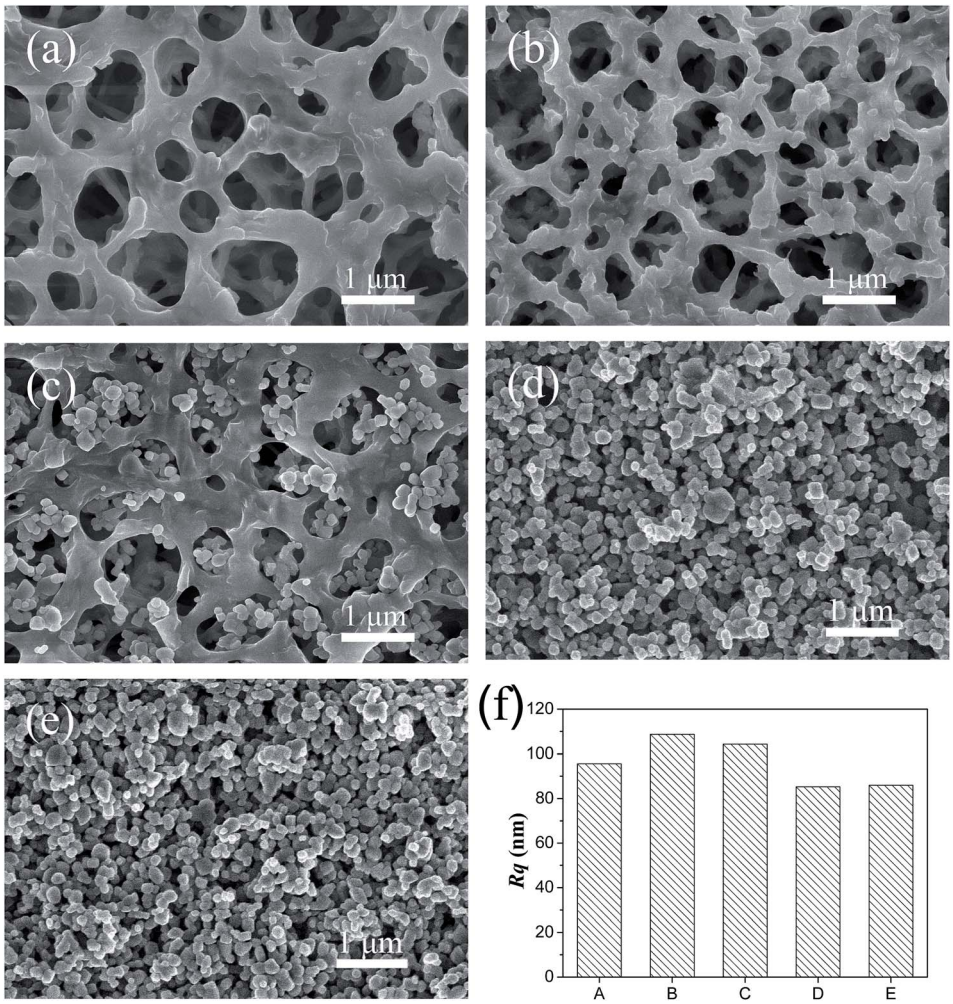

Fig. 2 SEM images of (a) pristine cellulose acetate membrane, (b) CS modified membrane, (c) CST (3 : 1) membrane, (d) CST (3 : 4) membrane, and (e) CST (3 : 7) membrane. (f) R_q values of different modified membranes: A – pristine cellulose acetate membrane, B – CS modified membrane, C – CST (3 : 1) membrane, D – CST (3 : 4) membrane, and E – CST (3 : 7) membrane.

the R_q value of the CST (3 : 4) modified membrane decreased to 85.30 nm, which indicated that the microscale roughness of the modified membrane was gradually lost as the hydrophilic TiO_2 nanoparticles increased. When the content of TiO_2 nanoparticles increased to 3.5 mg, the surface roughness was nearly unchanged with the R_q value of 85.90 nm. The relationship between surface roughness and membrane surface wettability will be discussed later.

X-ray photoelectron spectroscopy (XPS) was used to analyze the surface chemical composition of the pristine cellulose acetate membrane and the modified membranes. As shown in Fig. 3a, the elements of carbon and oxygen were examined on the pristine cellulose acetate membrane, while a weak N 1s peak at 399.9 eV was existent on the CS and CST modified membranes, which should arise from chitosan and the cross-linking agent glutaraldehyde. A strong Ti 2p peak was evident on the CST modified membranes, indicating that the TiO_2 nanoparticles were successfully coated. The element contents of different membranes were presented in Table S1.† The high-resolution spectra of C 1s peak showed four sub-peak at 285.0 eV, 286.3 eV, 287.2 eV and 288.9 eV, which were assigned to the $-CH_x$(C–C and C–H), C═N, C–O and O–C═O bonds, respectively (Fig. 3b).[25] As shown in Fig. 3c, a high-resolution spectra of N 1s peak was observed at 399.4 eV. The Ti 2p exhibited two distinct peaks at 458.1 eV of Ti $2p_{3/2}$ and at 464.0 eV of Ti $2p_{1/2}$ (Fig. 3d). Furthermore, the CST (3 : 4) membrane was measured by EDS mapping to investigate surface element composition. As shown in Fig. S3,† the EDS mapping results indicated that Ti, O, C and N were uniformly distributed on the membrane surface.

3.2 Wettability of membrane

To achieve effective oil/water separation, a membrane surface with stable superhydrophilic and underwater superoleophobic properties is critical. To evaluate the wettability of the pristine and modified membranes, both water contact angle (WCA) in air and underwater oil contact angle (OCA) were measured. As can be seen in Fig. 4a, the pristine cellulose acetate membrane showed a WCA of 82.5 ± 5.0°, which is not suitable for oil/water

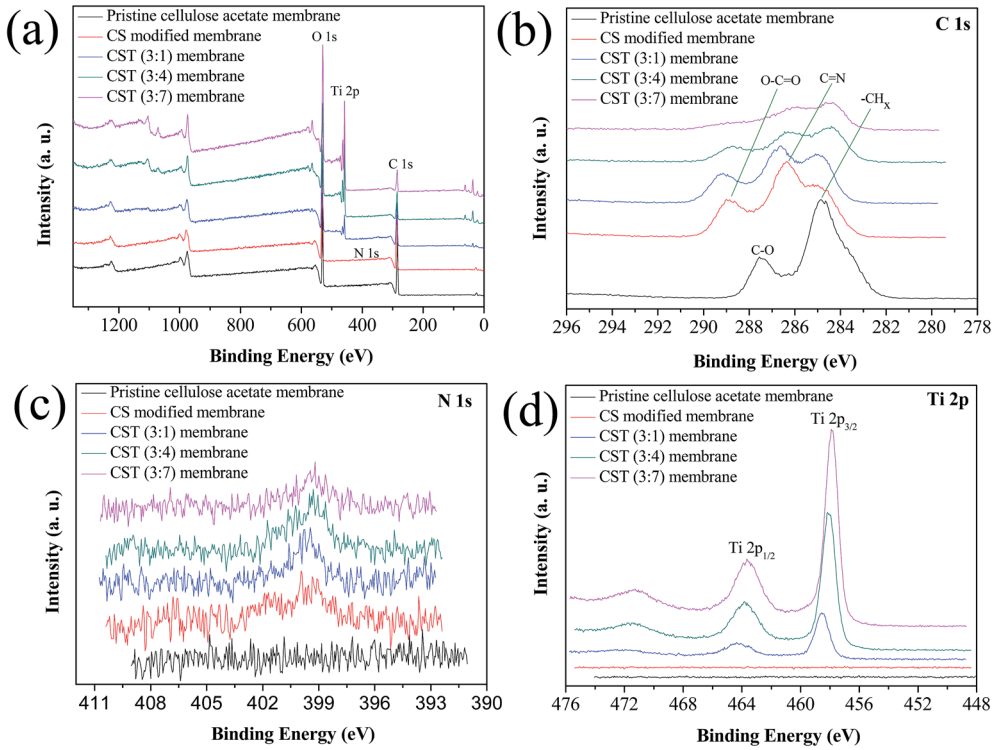

Fig. 3 (a) XPS survey spectra of the pristine cellulose acetate membrane and the modified membranes, and the corresponding high-resolution spectra of (b) C 1s, (c) N 1s and (d) Ti 2p.

separation. The CS modified membrane had a water contact angle of 69.2 ± 4.7°, due to the amine groups present in chitosan, which is hydrophilic. With the increase of TiO_2 nanoparticles, the WCA decreased rapidly. It can be seen that the WCA was nearly 0° within several seconds with the mass ratio of CS/TiO_2 of 3 : 4 and 3 : 7, indicating their superhydrophilicity. Underwater oil (take 1,2-dichloroethane as an example) contact angles can be utilized to evaluate the underwater oleophobic properties of different membranes. As shown in Fig. 4b, the pristine cellulose acetate membrane showed an underwater contact angle of 112.5 ± 3.8° and oil can easily adhere to the membrane, leading to membrane clogging. The CS modified membrane had a OCA of 139.2 ± 4.7°, and the relatively weak underwater oleophobic property cannot meet the requirement of oil/water separation. When the mass ratio of CS/TiO_2 was 3 : 1, the OCA of the modified membrane was 155.7 ± 3.3°. With the increase of hydrophilic TiO_2 nanoparticles, the underwater oil contact angles from 161.1 ± 4.5° for the CST (3 : 4) membrane to 165.7 ± 5.0° for the CST (3 : 7) membrane. The CST (3 : 4) and CST (3 : 7) modified membranes showed typical superhydrophilicity in air and underwater superoleophobic properties. The architecture of the hydrophilic TiO_2 contributed to hierarchical nanostructures and higher water capture capacity. It is usually accepted that hierarchical nanostructures and surface hydrophilicity of membrane surfaces synergistically contributed superhydrophilic and underwater superoleophobic properties.[17] Comparing the contact angles of the pristine cellulose acetate membrane and the CS modified membrane, we can conclude that the hydroxyl and amino functional groups

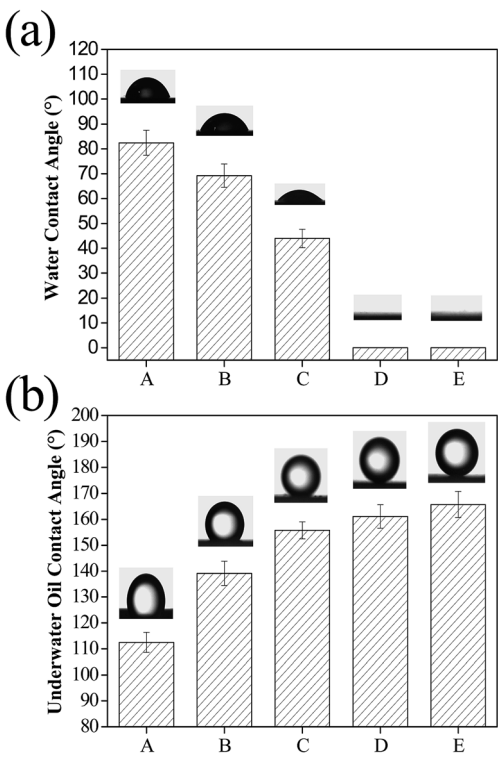

Fig. 4 (a) Water contact angle of different modified membranes and (b) underwater oil (1,2-dichloroethane) contact angle of different modified membranes: A – the pristine cellulose acetate membrane, B – CS modified membrane, C – CST (3 : 1) membrane, D – CST (3 : 4) membrane and E – CST (3 : 7) membrane.

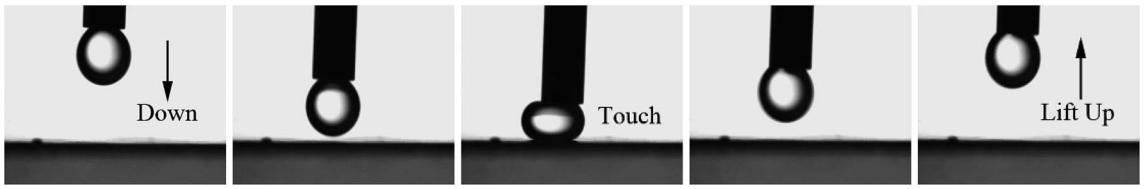

Fig. 5 Underwater oil-adhesion test of the CST (3 : 4) membrane. An oil droplet (1,2-dichloroethane, 2 μL) was contacted with the membrane surface, and then allowed to lift up.

on the chitosan and the geometrical structure synergistically improved the wettability of the membrane surface. With the addition of TiO_2 nanoparticles, surface roughness is reduced, but the improvement of membrane surface wettability is obvious. Therefore, the superhydrophilic TiO_2 nanoparticles played a key role in membrane surface hydrophilicity. Thus, the excellent wetting with superhydrophilicity and underwater superoleophobicity of the modified membrane is obtained by the synergistic effect of the outstanding hydration capacity of TiO_2 nanoparticles and hierarchical nanostructures. We also measured the contact angle of oil droplets in air. Contrary to our expectations, the oil (1,2-dichloroethane, 2 μL) contact angle in air was close to 0° for the CST (3 : 4) membrane, as presented in Fig. S4.† We believe that the cause of the CST (3 : 4) membrane superhydrophilicity and superoleophilicity in air is the intrinsic high surface energy and the micro/nanoscale hierarchical structures, which significantly amplify wettability.

To further investigate the oil repellent property of the membrane, the CST (3 : 4) membrane was selected as a suitable sample for an underwater oil-adhesion test. The underwater oil-adhesion test was dynamically measured using a 1,2-dichloroethane oil droplet (2 μL) on the needle tip of a microsyringe to contact with the CST (3 : 4) membrane and then leave the surface of the modified membrane. As can be seen in Fig. 5, an oil droplet was compressed on the membrane surface from a spherical to an ellipsoidal shape, and then leaves the surface of the CST (3 : 4) membrane easily. It can be seen from the image that the oil droplet can overcome the adhesion force with the CST (3 : 4) membrane, and the oil droplet exhibited almost no obvious deformation. In addition, there was no residue on the surface of the membrane. This result demonstrated that the underwater oil-adhesion force is extremely low, and simultaneously showed that the CST membrane has a superior anti-oil-fouling property.

3.3 Separation of oil-in-water emulsions by the modified membranes

To test the separating capacities of the pristine and modified membranes for oil-in-water emulsions, a series of proof-of-concept studies were performed. Cyclic oil/water separation tests were conducted using a vacuum filtration setup with a membrane permeation area of 12.56 cm^2. Prior to the separation process, the membrane was wetted by water and then sandwiched between two glass devices. The separation process for oil-in-water emulsion is simple. When the vacuum pump's switch was turned on, 50 mL of oil-in-water emulsion was separated by the modified CST membrane under a pressure difference of 0.09 MPa. After each surfactant-stabilized emulsion separation experiment, the used membranes were rinsed with water. The permeate flux F (L m^{-2} h^{-1}) was calculated by using eqn (1):

$$F = \frac{V}{At} \quad (1)$$

where V (L) is the volume of the oil-in-water emulsion; A (m^2) is the effective membrane area; and t is the time of the permeation experiment. The oil rejection coefficient R (%) was calculated by eqn (2):

$$R = \left(1 - \frac{C_P}{C_0}\right) \times 100\% \quad (2)$$

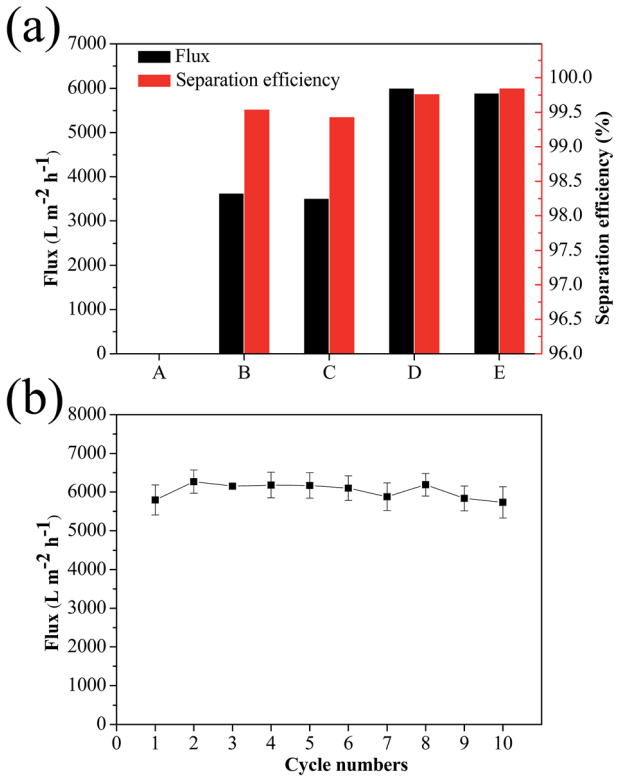

Fig. 6 (a) Flux and separation efficiency of different membranes for separation hexadecane-in-water: A – pristine cellulose acetate membrane, B – CS modified membrane, C – CST (3 : 1) membrane, D – CST (3 : 4) membrane, and E – CST (3 : 7) membrane. (b) Changes of flux of CST (3 : 4) membrane with increasing cycle numbers for separation.

where C_0 and C_P are the concentration of oil in the original oil-in-water emulsions and the permeate solution, respectively. The oil content of permeate was determined by an infrared spectrometer oil content analyzer (Oil 460, Beijing China Invent Instrument Tech. Co., Ltd., Beijing, China).

The flux and oil rejection coefficient of the pristine and the modified membranes for hexadecane-in-water emulsion are shown in Fig. 6a. It should be pointed out that the flux of emulsion was the average velocity for several cycles. 50 mL hexadecane-in-water emulsion cannot permeate and pass through the pristine cellulose acetate membrane, indicating its weak anti-oil-fouling performance (Video S1†). It can be seen that the CST (3 : 4) membrane had the highest flux of 6002.5 L m^{-2} h^{-1}, which is one order of magnitude higher than conventional filtration membranes (Table S2†).[34–38] When the mass ratio of chitosan and TiO_2 increased to 3 : 7, the flux decreased to 5893.7 L m^{-2} h^{-1} due to the increase of the thickness of the membrane by the Hagen–Poiseuille equation, in which the fluid dynamic theory suggests that the filtration flux inverses ratio to the thickness of the membrane.[39] All modified membranes exhibited extremely high oil rejection ratios: 99.54% for the chitosan modified membrane, 99.43% for the CST (3 : 1) membrane, 99.77% for the CST (3 : 4) membrane, and 99.85% for the CST (3 : 7) membrane. The recycle numbers of different membranes for hexadecane-in-water emulsion separation were shown in Fig. S5.† Herein, when the flux is less than 500 L m^{-2} h^{-1}, it can be seen that the membrane is not available. The CST (3 : 4) membrane had the highest separation cycles, *i.e.*, over 10 repetitions. This result was consistent with the contact angles, as presented in Fig. 4a and b. Considering the excellent wettability and high flux for hexadecane-in-water emulsion separation, the CST (3 : 4) membrane was chosen for further investigation. As can be seen in Fig. 6b, the CST (3 : 4) membrane retained its high flux even after 10 separation cycles. To characterize the loss of TiO_2 nanoparticles, the surface morphology of the CST (3 : 4) membrane after 10 separation cycles for hexadecane-in-water emulsion was observed by SEM. As clearly presented in Fig. S6,† there was only a slight loss of TiO_2 nanoparticles due to the wash with water.

A schematic diagram of the hexadecane-in-water emulsion separation process of the CST (3 : 4) membrane was achieved, as shown in Fig. 7a–c. The prepared CST (3 : 4) membrane was pre-wetted by water and fixed between two glass devices (Fig. 7a), and then the hexadecane-in-water emulsion was poured onto the modified membrane (Fig. 7b). As shown in Fig. 7c, when the

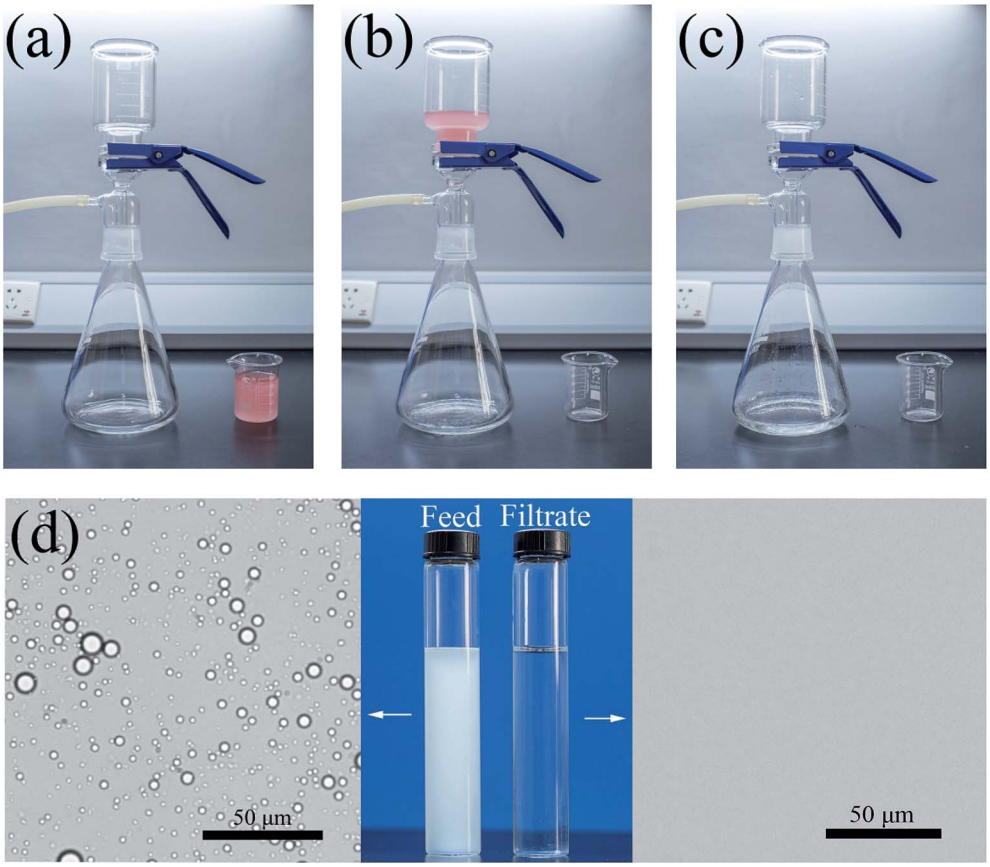

Fig. 7 (a–c) Schematic diagram of the hexadecane-in-water emulsion separation process of the CST (3 : 4) membrane. (a) The pre-wetted CST (3 : 4) membrane was sandwiched between two glass devices, and the hexadecane-in-water emulsion remained stable. (b) The hexadecane-in-water emulsion was poured onto the modified membrane. (c) Water permeated through the CST (3 : 4) membrane, while hexadecane stayed on the membrane surface. (d) Optical microscopy images and digital photos of the hexadecane-in-water emulsion separation process: before separation (left) and after separation (right).

vacuum pump's switch was turned on, hexadecane (dyed with oil red O) was repelled by the membrane, while the water quickly permeated through the membrane (Video S2†). No visible oil was seen in the permeate solution due to the super-hydrophilic and underwater superoleophobic properties of the CST (3 : 4) membrane. Clearly revealed by the images shown in Fig. 7d, original oil-in-water emulsion has a milky white color prior to treatment, while the collected filtrate was colorless and transparent. In addition, we also observed droplets that existed in the feed of the hexadecane-in-water emulsion and the filtrate by optical microscopy. As clearly shown in Fig. 7d, oil droplets in the feed solution were homogeneously dispersed in the whole view, while no droplets can be seen in the whole view of the collected permeate, confirming that this CST (3 : 4) membrane was highly efficient for separating hexadecane-in-water emulsion. The oil droplet size distribution of hexadecane-in-water emulsion in feed was measured by dynamic light scattering (DLS). As presented in Fig. S7,† the droplet size of the hexadecane-in-water emulsion is in the range of 1.4 μm to 2.1 μm, with a mean size of 1.7 μm.

Three other sodium dodecyl sulfonate (SDS) stabilized oil-in-water emulsions were utilized to measure the separation capacity of the CST (3 : 4) membrane, including octane-in-water, petroleum ether-in-water, and toluene-in-water. As can be seen in Fig. S8,† all of the surfactant stabilized emulsions exhibited extremely high fluxes: 5517.43 L m^{-2} h^{-1} for octane-in-water, 4521.01 L m^{-2} h^{-1} for petroleum ether-in-water, and 3644.63 L m^{-2} h^{-1} for toluene-in-water, while the oil rejection ratios were 98.46%, 97.72% and 97.06%, respectively. The oil concentration of each kind of oil-in-water emulsion was lower than 20 mg L^{-1}, which can satisfy the U.S. Environmental Protection Agency (EPA)'s regulation that the maximum discharge of grease and oil in effluents is 42 mg L^{-1} for any one day. In addition, water trapped in the micro/nanoscale hierarchical structure to form a continuous phase provided a strong oil repelling force, which is essential for oil-in-water emulsion separation. Moreover, the adsorbed water layer provided channels for water droplets from the oil-in-water emulsion to permeate into the opposite side of the modified membrane. Thus, the oil-in-water emulsions were separated successfully due to the thin water layer that can prevent oil droplets from passing through the modified membrane. When the membrane had a high water capture capacity, it can form a strong water layer on the oil/water/membrane contact interface to prevent oil droplets from contacting with the membrane surface and maintain the stable underwater superoleophobicity of the membrane.

3.4 Stability of the modified membrane

As is well known, oily wastewater sometimes exists in corrosive acid, alkali, or saline environments. For a water-removing membrane, during the emulsion separation process, the membrane surface is full of water, and the durability and stability of the materials in those corrosive solutions would be critical to maintain superhydrophilicity and underwater superoleophobicity. To evaluate stability, we further monitored the underwater oil contact angles after immersing the CST (3 : 4) membrane in a series of solutions with various pH values (from 1 to 13). It can be seen that the underwater oil (1,2-dichloroethane) contact angles of the modified membrane >150° (Fig. 8a), indicating underwater superoleophobicity under a strong acid and alkali environment. Moreover, as shown in Fig. 8b, the oil contact angle of the CST (3 : 4) membrane was hardly affected by the salt concentration, and all of the OCA > 150°. Fig. S9† showed the SEM images of the CST (3 : 4) membrane after immersing in different solutions (pH = 1, pH = 13 and 5% NaCl). As clearly presented in Fig. S9a–c,† there were no obvious change for the surface morphology of the CST (3 : 4) membrane in those corrosive solutions.

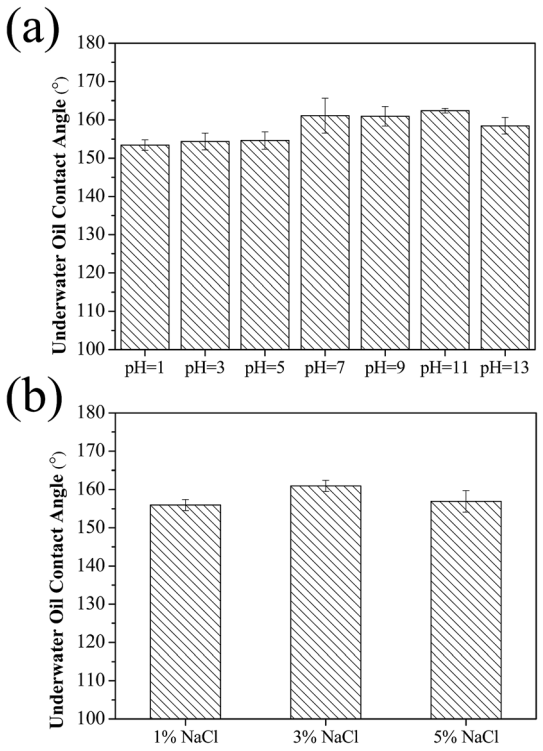

Fig. 8 Underwater oil contact angles of the CST (3 : 4) membrane under different (a) pH and (b) salt concentrations.

Furthermore, the separation performances for hexadecane-in-corrosive liquid emulsions with pH of 1, 13, and 5% NaCl were investigated to evaluate stability of the CST (3 : 4) membrane. As shown in Fig. S10,† the separation fluxes for hexadecane-in-water at pH = 1, pH = 13, and 5% NaCl were 5094.63 L m^{-2} h^{-1}, 5215.06 L m^{-2} h^{-1}, and 4282.8 L m^{-2} h^{-1}, respectively. Moreover, the oil rejection ratios of the CST (3 : 4) membrane hexadecane-in-corrosive liquid emulsions were higher than 99%. The decline of separation performances for the CST (3 : 4) membrane was not obvious, and the CST (3 : 4) membrane was stable. These results demonstrated that the CST (3 : 4) membrane possesses advantages for industrial applications.

4. Conclusions

We have successfully fabricated a novel chitosan–TiO_2 composite membrane with robust superhydrophilic in air and

underwater superoleophobic properties by the filtration technique under a vacuum filtration device. The modified CST membrane combined the benefits of both chitosan and TiO_2 in a synergistic manner. The resulting membrane displays superior oil/water separation efficiency above 97% and a high permeate flux above 6000 L m^{-2} h^{-1} for hexadecane-in-water emulsion, which is several times greater than conventional filtration membranes. The characteristic of hydrophilic TiO_2 endows the CST membrane with excellent anti-oil-fouling and low oil-adhesion properties, indicating the potential application of the modified membrane for removing emulsified oil in industrial contexts. More importantly, the CST membrane possesses superior chemical stability and outstanding resistance to strong acid, alkali, and salt. Therefore, we expect that this work would be substantially helpful for the development and design of new anti-oil fouling materials and related devices.

Conflicts of interest

There are no conflicts to declare.

Acknowledgements

This work was supported by the National Natural Science Foundation of China (Grant no. 21677087).

References

1 M. Cheryan and N. Rajagopalan, *J. Membr. Sci.*, 1998, **151**, 13–28.
2 N. Cao, Q. Lyu, J. Li, Y. Wang, B. Yang, S. Szunerits and R. Boukherroub, *Chem. Eng. J.*, 2017, **326**, 17–28.
3 K. Suresh, T. Srinu, A. K. Ghoshal and G. Pugazhenthi, *RSC Adv.*, 2016, **6**, 4877–4888.
4 S. Zhang, F. Lu, L. Tao, N. Liu, C. Gao, L. Feng and Y. Wei, *ACS Appl. Mater. Interfaces*, 2013, **5**, 11971–11976.
5 H. Yoon, S. H. Na, J. Y. Choi, S. S. Latthe, M. T. Swihart, S. S. Al-Deyab and S. S. Yoon, *Langmuir*, 2014, **30**, 11761–11769.
6 A. Al-Shamrani, A. James and H. Xiao, *Water Res.*, 2002, **36**, 1503–1512.
7 S. Maphutha, K. Moothi, M. Meyyappan and S. E. Iyuke, *Sci. Rep.*, 2013, **3**, 1509.
8 W. Zhang, X. Chen, J. Pan, C. Gao and J. Shen, *RSC Adv.*, 2016, **6**, 114750–114757.
9 Z. Xue, Y. Cao, N. Liu, L. Feng and L. Jiang, *J. Mater. Chem. A*, 2014, **2**, 2445–2460.
10 B. Li, X. Liu, X. Zhang and W. Chai, *Eur. Polym. J.*, 2015, **73**, 374–379.
11 Y. Cao, X. Zhang, L. Tao, K. Li, Z. Xue, L. Feng and Y. Wei, *ACS Appl. Mater. Interfaces*, 2013, **5**, 4438–4442.
12 X. Zheng, Z. Guo, D. Tian, X. Zhang, W. Li and L. Jiang, *ACS Appl. Mater. Interfaces*, 2015, **7**, 4336–4343.
13 Z. Xue, S. Wang, L. Lin, L. Chen, M. Liu, L. Feng and L. Jiang, *Adv. Mater.*, 2011, **23**, 4270–4273.
14 T. Shen, S. Li, Z. Wang and L. Wang, *RSC Adv.*, 2016, **6**, 115196–115203.
15 N. Liu, M. Zhang, W. Zhang, Y. Cao, Y. Chen, X. Lin, L. Xu, C. Li, L. Feng and Y. Wei, *J. Mater. Chem. A*, 2015, **3**, 20113–20117.
16 X. Lin, Y. Chen, N. Liu, Y. Cao, L. Xu, W. Zhang and L. Feng, *Nanoscale*, 2016, **8**, 8525–8529.
17 X. Zhao, Y. Su, Y. Liu, Y. Li and Z. Jiang, *ACS Appl. Mater. Interfaces*, 2016, **8**, 8247–8256.
18 F. Al-Sagheer and S. Merchant, *Carbohydr. Polym.*, 2011, **85**, 356–362.
19 Y. Haldorai and J. J. Shim, *Polym. Compos.*, 2014, **35**, 327–333.
20 J. P. Chaudhary, N. Vadodariya, S. K. Nataraj and R. Meena, *ACS Appl. Mater. Interfaces*, 2015, **7**, 24957–24962.
21 B. D. McCloskey, H. Ju and B. D. Freeman, *Ind. Eng. Chem. Res.*, 2009, **49**, 366–373.
22 T. C. Mokhena and A. S. Luyt, *J. Cleaner Prod.*, 2017, **156**, 470–479.
23 J. Yang, H. Song, X. Yan, H. Tang and C. Li, *Cellulose*, 2014, **21**, 1851–1857.
24 J. J. Wang, Z. W. Zeng, R. Z. Xiao, T. Xie, G. L. Zhou, X. R. Zhan and S. L. Wang, *Int. J. Nanomed.*, 2011, **6**, 765–774.
25 J. Y. Huang, S. H. Li, M. Z. Ge, L. N. Wang, T. L. Xing, G. Q. Chen, X. F. Liu, S. S. Al-Deyab, K. Q. Zhang, T. Chen and Y. K. Lai, *J. Mater. Chem. A*, 2015, **3**, 2825–2832.
26 B. Y. L. Tan, M. H. Tai, J. Juay, Z. Liu and D. Sun, *Sep. Purif. Technol.*, 2015, **156**, 942–951.
27 O. A. Monteiro and C. Airoldi, *Int. J. Biol. Macromol.*, 1999, **26**, 119–128.
28 P. S. Brown and B. Bhushan, *Sci. Rep.*, 2015, **5**, 8701.
29 T. Sun, L. Feng, X. Gao and L. Jiang, *Acc. Chem. Res.*, 2005, **38**, 644–652.
30 Q. Wang, Y. Fu, X. Yan, Y. Chang, L. Ren and J. Zhou, *Appl. Surf. Sci.*, 2017, **412**, 10–18.
31 X. Zhang, F. Shi, J. Niu, Y. Jiang and Z. Wang, *J. Mater. Chem.*, 2008, **18**, 621–633.
32 Y. Xiu, L. Zhu, D. W. Hess and C. Wong, *Nano Lett.*, 2007, **7**, 3388–3393.
33 A. Cassie, *Discuss. Faraday Soc.*, 1948, **3**, 11–16.
34 T. Yuan, J. Meng, T. Hao, Y. Zhang and M. Xu, *J. Membr. Sci.*, 2014, **470**, 112–124.
35 P. Gao, Z. Liu, D. D. Sun and W. J. Ng, *J. Mater. Chem. A*, 2014, **2**, 14082.
36 B. Chakrabarty, A. Ghoshal and M. Purkait, *J. Membr. Sci.*, 2008, **325**, 427–437.
37 X. Hu, Y. Yu, J. Zhou, Y. Wang, J. Liang, X. Zhang, Q. Chang and L. Song, *J. Membr. Sci.*, 2015, **476**, 200–204.
38 H. Shi, Y. He, Y. Pan, H. Di, G. Zeng, L. Zhang and C. Zhang, *J. Membr. Sci.*, 2016, **506**, 60–70.
39 X. Peng, J. Jin, Y. Nakamura, T. Ohno and I. Ichinose, *Nat. Nanotechnol.*, 2009, **4**, 353–357.

